

Ionic transport studies of the glassy silver vanadomolybdate system

B. V. R. CHOWDARI, R. GOPALAKRISHNAN, S. H. GOH*, K. L. TAN

*Department of Physics, and *Department of Chemistry, National University of Singapore, Singapore 0511*

Ionic conductivity of the $\text{Ag}_2\text{O}-\text{MoO}_3-\text{V}_2\text{O}_5$ system has been studied over a wide range of frequency, temperature and composition. A narrower glass forming region has been found in comparison to the corresponding $\text{Ag}_2\text{O}-\text{MoO}_3-\text{P}_2\text{O}_5$ and $\text{Ag}_2\text{O}-\text{B}_2\text{O}_3-\text{P}_2\text{O}_5$ systems. The highest conductivity at room temperature, $\sigma_{\text{rt}} = 3.21 \times 10^{-6} \Omega^{-1} \text{cm}^{-1}$ (d.c.) with an activation energy, E_{act} , of 0.466 eV, was observed for the glass former's ratio of unity. Further, it reached a maximum value of $2.2 \times 10^{-2} \Omega^{-1} \text{cm}^{-1}$ with $E_{\text{act}} = 0.153$ eV when the oxide-base glass was dissolved with AgI. D.c. conductivity, hopping rate and relaxation time in the present system have been found to be characterized by the same activation energy.

1. Introduction

Inorganic oxide glasses are of commercial importance due to their structural versatility and, among them, fast ion conducting glasses have been of scientific interest for many years as solid electrolytes. The structural modifications in the oxide glass formers such as P_2O_5 , B_2O_3 , V_2O_5 , etc., are known to induce notable changes in physical properties of the glasses. Recently more complex glasses have been synthesized by dissolved mineral salts in oxide-base glasses [1-4]. With the aim of exploring the effect of mixed glass formers on ionic transport, an investigation of the thermal, electrical and electrochemical properties of undoped and AgI-doped $\text{Ag}_2\text{O}-\text{MoO}_3-\text{V}_2\text{O}_5$ system has been undertaken. As both V_2O_5 and MoO_3 are conditional glass formers and hence their glass forming ability with Ag_2O is very limited, the studies on this mixed glass forming system will be of great interest. The results obtained from these studies are reported here.

2. Synthesis and characterization of glasses

2.1. Preparation

The glasses are obtained by direct synthesis from mixtures of appropriate proportions of NH_4VO_3 , AgNO_3 , MoO_3 and AgI taken in mol %. The mixtures were crushed into powder, placed in a platinum crucible and melted in the temperature range 1173 to 1573 K. The melt was then quenched by quickly pouring into a mould to yield 13 mm diameter and 1 mm thick samples. Glasses of various compositions are labelled by the following parameters

$$x = (\text{AgI})/[(\text{AgI}) + (\text{Ag}_2\text{O})]$$

$$y = (\text{V}_2\text{O}_5)/[(\text{V}_2\text{O}_5) + (\text{MoO}_3)]$$

and

$$n = [(\text{V}_2\text{O}_5) + (\text{MoO}_3)]/(\text{Ag}_2\text{O})$$

For example, glass G3 labelled $n = 1$, $y = 0.5$ is

realized by taking $(0.499) \times$ (molecular weight of Ag_2O) grams of Ag_2O , $(0.249) \times$ (molecular weight of MoO_3) grams of MoO_3 and $(0.249) \times$ (molecular weight of V_2O_5) grams of V_2O_5 . It is labelled $n = 1$, $y = 0.5$, because $(0.249 + 0.249)/0.499 = 1$, and $0.249/(0.249 + 0.249) = 0.5$, respectively. All the glasses were transparent, but dark brown in colour.

2.2. Glass transformation temperature (T_g)

The glass transition temperature was determined by using a Perkin-Elmer DSC-4 differential scanning calorimeter.

A sample weighing 10 to 20 mg was crimped in an aluminium sample pan and scanned using a heating rate of $20^\circ \text{C min}^{-1}$. Fig. 1a shows the vitreous domain in the undoped ternary system. As shown in Table I, T_g is found to increase when MoO_3 is systematically replaced by V_2O_5 in the range $y = 0.2$ to 0.6. A further increase in y seems to cause a slight reduction in T_g . A narrow glass forming region was found in the $\text{Ag}_2\text{O}-\text{MoO}_3-\text{V}_2\text{O}_5$ system in comparison to the borophosphate [5] and molybdophosphate [6] systems. As will be evident later, G3 has the highest conductivity at room temperature and hence it is doped with AgI to enhance it further. Fig. 1b represents the glass forming region when G3 ($n = 1$, $y = 0.5$) is systematically doped with AgI. As can be seen from Fig. 1c and Table I, T_g decreases drastically as more and more AgI is incorporated into the glassy matrix. Drastic changes in the AgI-doped system compared to that system which contains glass modifier (Ag_2O) alone, could be explained by the fact that AgI plays the role of a plasticizer facilitating the co-operative chain movement [7]. The crystallization temperature (T_c) was found to vary with both the heating rate and composition. T_g was found to be higher in G10 (0.23 $\text{Ag}_2\text{O}-0.115 \text{ MoO}_3-0.115 \text{ V}_2\text{O}_5-0.538 \text{ AgI}$ (mol %)) compared to the corresponding highly conducting silveriodomolybdate glass [8].

TABLE I Some characteristic parameters of the undoped and AgI-doped glassy $\text{Ag}_2\text{O}-\text{MoO}_3-\text{V}_2\text{O}_5$ ternary system

Glass no.	Composition (mol %)			Parameters			T_g ($^{\circ}\text{C}$)	σ_{it} ($\Omega^{-1}\text{cm}^{-1}$)	σ_0	Activation energy (eV) from		K' ($10^9 \Omega^{-1}\text{cm}^{-1}\text{Hz}^{-1}\text{k}$)	τ_c at room temp (sec)
	Ag_2O	MoO_3	V_2O_5	AgI	n	γ				x	$\sigma_{d.c.}$		
G1	0.499	0.399	0.099	0	1	0.2	0	4.77×10^{-7}					
G2	0.499	0.299	0.199	0	1	0.4	0	1.01×10^{-6}					
G3	0.499	0.249	0.249	0	1	0.5	0	3.21×10^{-6}	14.26	0.466			
G4	0.499	0.199	0.299	0	1	0.6	0	1.27×10^{-6}					
G5	0.499	0.099	0.399	0	1	0.8	0	6.60×10^{-7}	0.032	0.239	0.171	0.27	1.46×10^{-5}
G6	0.473	0.236	0.236	0.052	1	0.5	0.1	1.71×10^{-5}					
G7	0.411	0.205	0.205	0.176	1	0.5	0.3	2.94×10^{-5}	0.915	0.245	0.282	0.25	2.97×10^{-8}
G8	0.374	0.187	0.187	0.25	1	0.5	0.4						
G9	0.333	0.166	0.166	0.333	1	0.5	0.5	2.56×10^{-4}					
G10	0.23	0.115	0.115	0.538	1	0.5	0.7	2.20×10^{-2}	4.61	0.153	0.156	0.157	2.45×10^{-9}
G11	0.166	0.083	0.083	0.666	1	0.5	0.8	5.82×10^{-3}		0.183			
G12	0.09	0.045	0.045	0.818	1	0.5	0.9	8.48×10^{-3}					
G13*	0.20	0.20	0	0.60	1	0.5	0.9	1.60×10^{-2}	10	0.173			

* From [8].

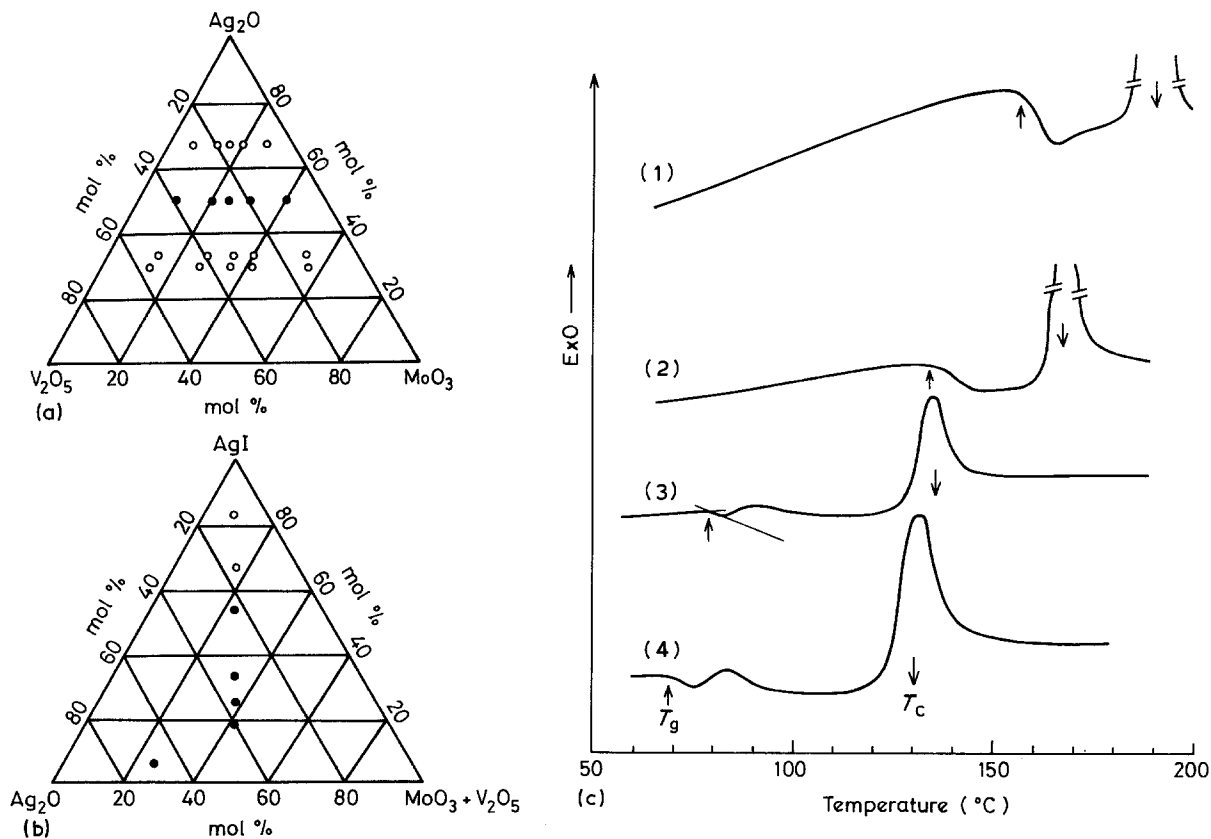


Figure 1 (a) Vitreous domain in the $\text{Ag}_2\text{O}-\text{MoO}_3-\text{V}_2\text{O}_5$ ternary system. (●) Glassy, (○) partially/fully crystallized. (b) Vitreous domain in the AgI -doped system. (c) DTA curves for (1) G6, (2) G8, (3) G10 with scan rate $20^\circ\text{C min}^{-1}$ and (4) G10 with scan rate $40^\circ\text{C min}^{-1}$. For actual composition refer to Table I.

3. Electrical properties

3.1. Experimental procedure

In order to have blocking electrodes, the polished flat surfaces of the samples were gold coated by thermal evaporation. The sample was spring loaded between the electrodes and the electrical conductivity was measured by the complex impedance technique using an HP 3575A gain-phase meter interfaced to an Apple IIe computer. The signal applied across the sample was 50 mV at any frequency. The frequency was varied from 10 Hz to 2 MHz over the temperature range 123 to 420 K. Further experimental details were published elsewhere [9, 10].

3.2. Conductivity results and analysis

A typical complex impedance diagram for a range of temperatures is shown in Fig. 2 for G6. It is evident that at each temperature the data are represented by a nearly perfect semicircular arc in the high-frequency region. The arc in the high-frequency region is known to arise due to the ionic migration in the bulk of the electrolyte [11]. The abscissa of the intersection of the low-frequency extrapolation of the semicircular arc (equals ohmic resistance) with the real axis has been used to calculate d.c. conductivity. The spikes observed at low frequencies arise from the interfacial capacitance. The small departure of the high-

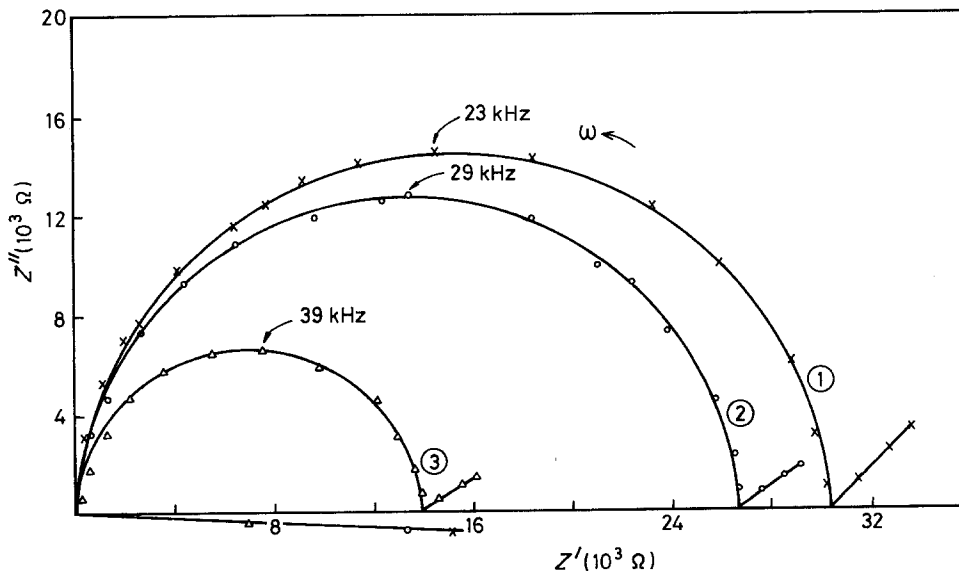


Figure 2 Impedance data for G6 at 1 (x) 313 K, 2 (o) 333 K and 3 (Δ) 353 K.

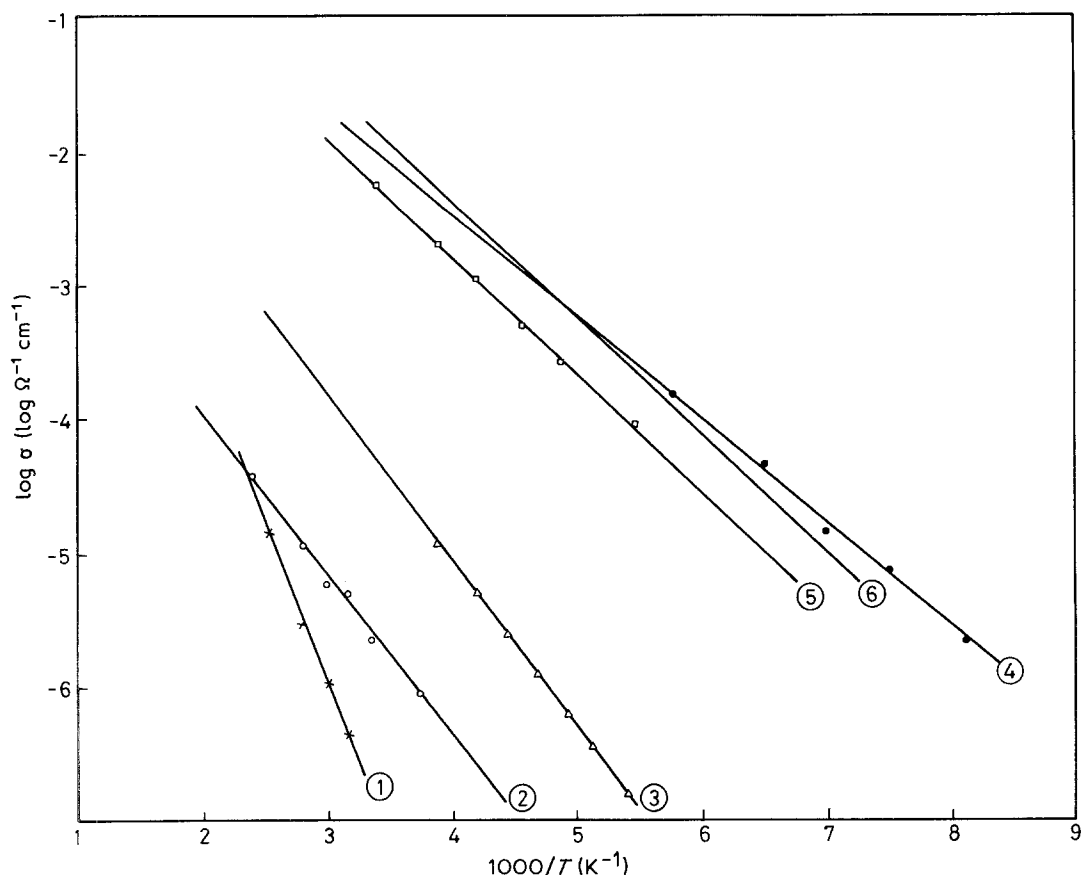


Figure 3 Plots of $\log \sigma$ against $1000/T$ for 1 (x) G3, 2 (o) G6, 3 (Δ) G8, 4 (\bullet) G10, 5 (\square) G11, and 6 G13.

frequency arc from the semicircular nature could be attributed to the multiple relaxation behaviour [12]. The bulk capacitance can be calculated using the expression $\omega RC = 1$ at Z''_{\max} where R is the bulk resistance and C is the bulk capacitance. The capacitance (C) is found to be $\sim 68\text{pF}$ at 353 K for G6. This larger capacitance could be attributed to the compactness of the glass.

The temperature dependence of the conductivity is shown in the Arrhenius form in Fig. 3. Linear least-square fits give the activation energy (E_{act}) and the pre-exponential factor (σ_0) in the Arrhenius equation for both the undoped and the AgI-doped systems. As is evident from Table I, ionic conductivity is found to vary with glass former ratio. The maximum ionic conductivity, $\sigma_{\text{ri}} = 3.21 \times 10^{-6} \Omega^{-1} \text{cm}^{-1}$, has been obtained when the glass former ratio is unity. This appears to be one order smaller in comparison to the corresponding borophosphate system [5]. This implies that the borophosphate glassy network is conveniently more modifiable than vanadomolybdate system by Ag_2O to give higher conductivity. Further, σ_{ri} increases by four orders of magnitude when doped systematically with AgI. Additional doping with AgI ($x > 0.7$) results in the partial crystallization of the sample with lower conductivity and higher activation energy in comparison to the corresponding values in G10. In comparison to the silver iodomolybdate glass (G13), a slight increase in σ_{ri} has been observed with lower activation energy and higher glass transition temperature. The lower activation energy may be due to the dissociation of solute AgI by an equilibrium type $\text{AgI} \rightleftharpoons \text{Ag}^+ + \text{I}^-$ in the glass matrix [13], similar

to an electrolyte weakly dissociated in a solvent. Hence $x = 0.7$ may be the limiting value for doping in G3 to reach a maximum conductivity ($2.2 \times 10^{-2} \Omega^{-1} \text{cm}^{-1}$), which is comparable with the other silver-ion conducting glass systems studied so far [14].

The frequency-dependant conductivity has been calculated using the formula $\sigma = \omega \epsilon_0 \epsilon''$ and the results for G6 at different temperatures are shown in Fig. 4. It can be seen that the low-temperature plots are characterized by a frequency-independent region in the low-frequency domain and a high conductivity dispersion in the high-frequency domain. The observation seen here could be explained by using Jonscher's universal expression [15]. Making use of the expression $K' = \sigma T / \omega_p$, defined by Almond *et al.* [16], the mobile ion concentration factor has been determined at various temperatures and compositions. The factor K' has been found to increase with AgI content and the hopping rate (ω_p) has been found to be thermally activated. E_{act} calculated from the Arrhenius plots of the characteristic frequencies (ω_p , shown in Fig. 4) are given in Table I. The K' factor has also been found to be nearly invariant in the temperature range studied for all compositions, as observed in other systems [17, 18].

3.3. Modulus analysis

The absence of a dielectric loss peak in the audio frequency range in the present doped glassy system, when measured at low temperatures, has led us to the complex electric modulus formalism for analysing the above data. Normalized modulus spectra obtained in the temperature range 113 to 123 K are shown in

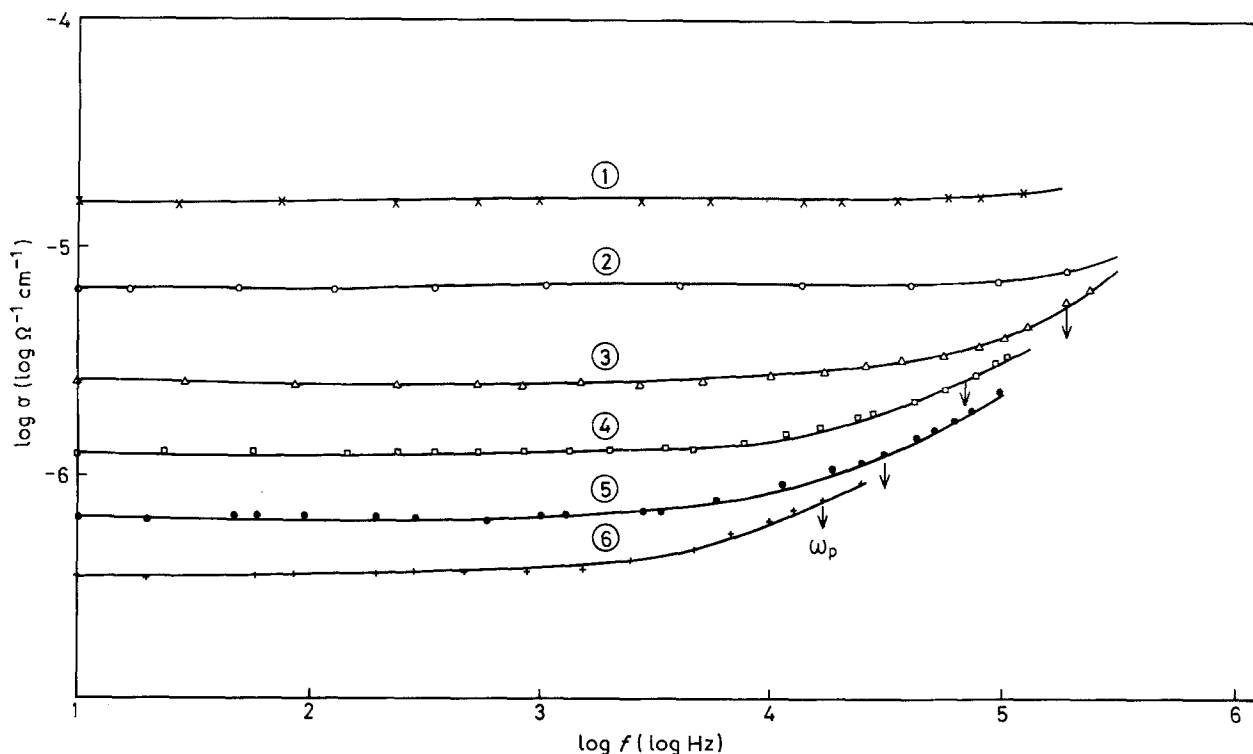


Figure 4 Plots of conductivity against frequency for G6 at 1 (x) 253 K, 2 (o) 240 K, 3 (Δ) 223 K, 4 (□) 213 K, 5 (●) 203 K and 6 (+) 193 K.

Fig. 5. Even though the characteristics such as width and the non-Debye nature of the modulus spectrum remains constant, the frequency corresponding to the peak of M'' increases with increase in temperature following the ionic glassy trend [19–21]. The activation energies calculated from the modulus data are given in Table I. Defining the relaxation time of the

system ($\tau_c = 1/2\pi f_c$) where f_c is the frequency of the M'' peak maxima, it can be seen at that at constant temperature, the relaxation time τ_c appears to be lower for higher AgI doping and vice versa. The values of f_c and ω_p for the AgI-doped glasses were plotted in an Arrhenius fashion and shown in Fig. 6. D.c. conductivity, hopping rate and relaxation time are found

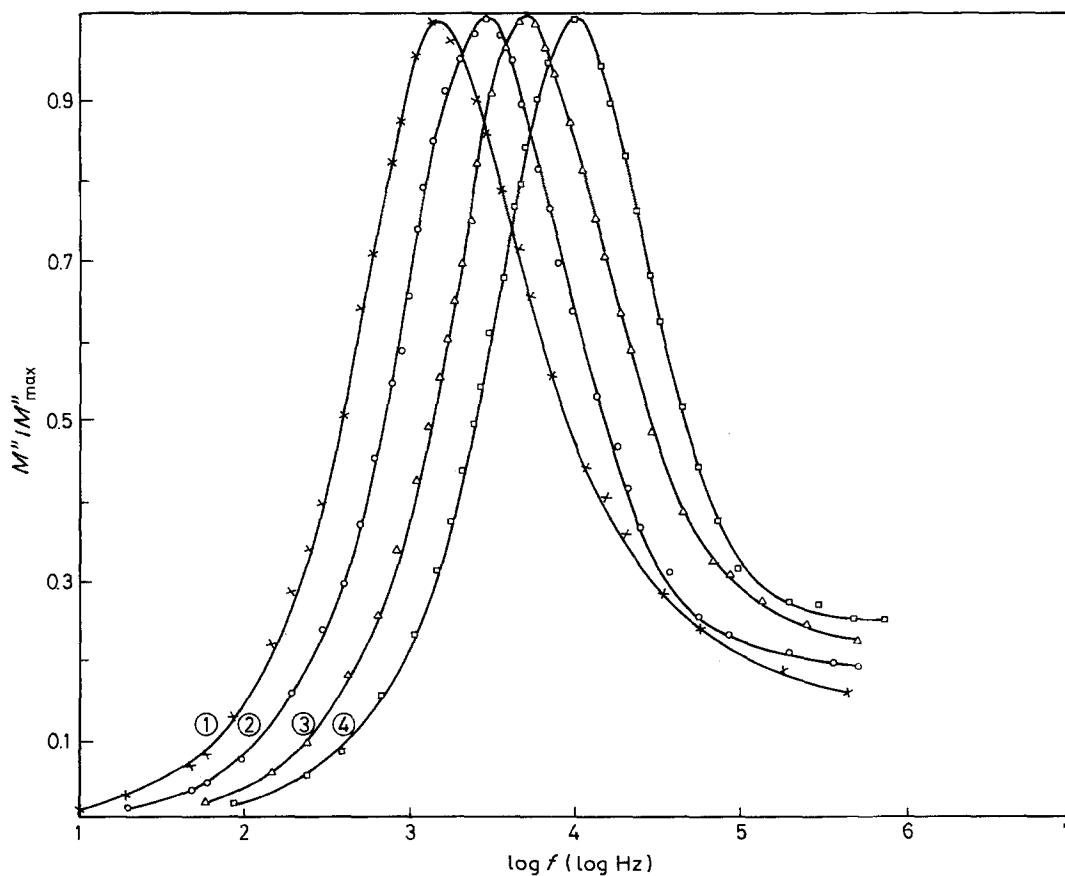


Figure 5 Normalized modulus spectrum for G8 at 1 (x) 193 K, 2 (o) 203 K, 3 (Δ) 213 K and 4 (□) 223 K.

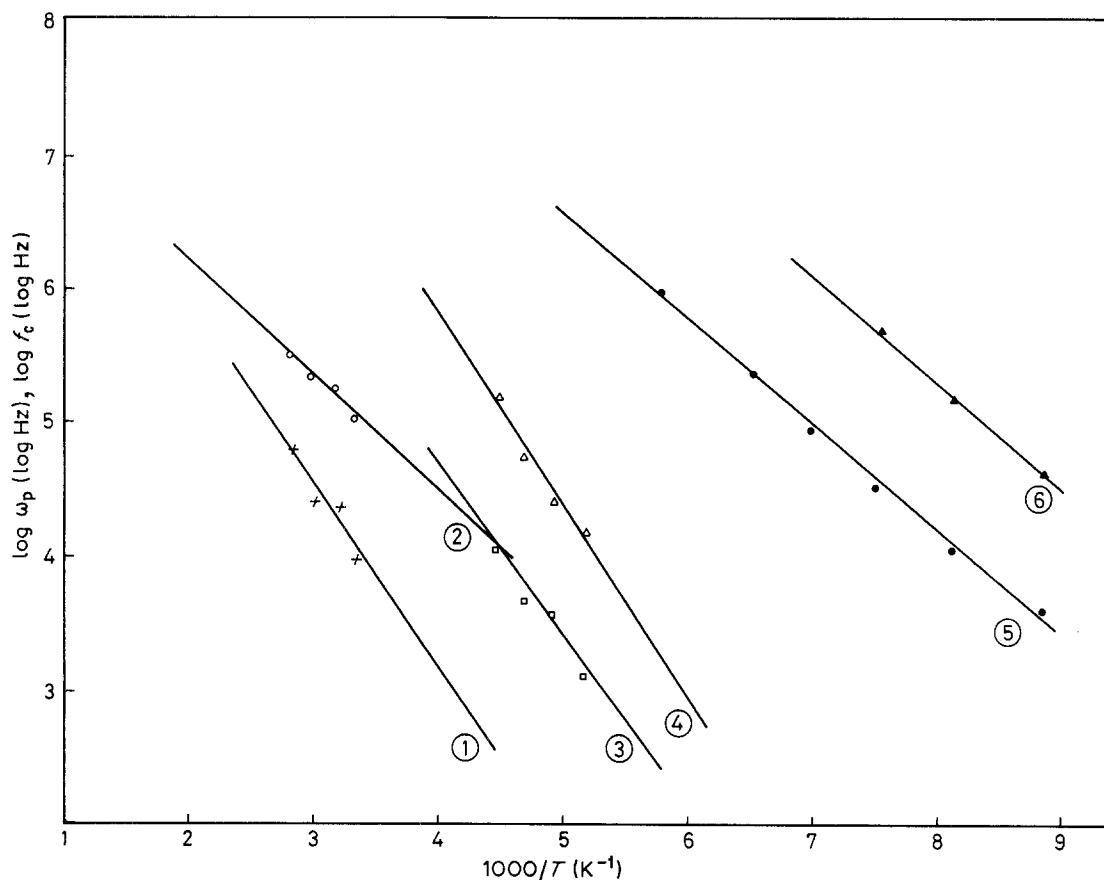


Figure 6 Plots of relaxation parameters against temperature for different compositions. Hopping rate (ω_p) for 2 (○) G6, 3 (□) G8 and 6 (▲) G10. Modulus peak frequencies (f_c) for 1 (x) G6, 4 (Δ) G8 and 5 (●) G10.

to have the same activation energy, which compares favourably with the values obtained for other AgI-based systems [22, 23].

4. Cell properties

The concept of an all-solid-state battery has been very promising and these batteries have been extensively investigated because of their advantages, e.g. long-shelf life, wide temperature range of operation, miniaturization, etc. Crystalline or glassy solid electrolyte-based electrochemical cells of Ag^+ ions have been studied in detail [24]. In the following section, the cell construction process and the discharge properties of an electrochemical cell using one of the presently investigated glasses (G10) as the solid electrolyte will be discussed.

4.1. Open circuit voltage

The open circuit voltages (OCV) were measured by using the cell configuration $\text{Ag}|\text{glassy electrolyte}|\text{I}_2, \text{C}$. The anode (silver powder), electrolyte (thin layer) and cathode [mixture of I_2 and carbon black (4:1 weight ratio)] were pressed together to form a pellet of 10 mm diameter. The cell was then sealed with epoxy resin. The OCV was measured by a high-impedance electrometer model 617 (Keithley). The transport number of Ag^+ ions measured by the e.m.f. method was found to be practically unity. The OCV was always found to be stable at 687 mV for more than 6 weeks.

4.2. Discharge curves

The discharge curve under a constant load resistance is shown in Fig. 7a. It is clear from the figure that the

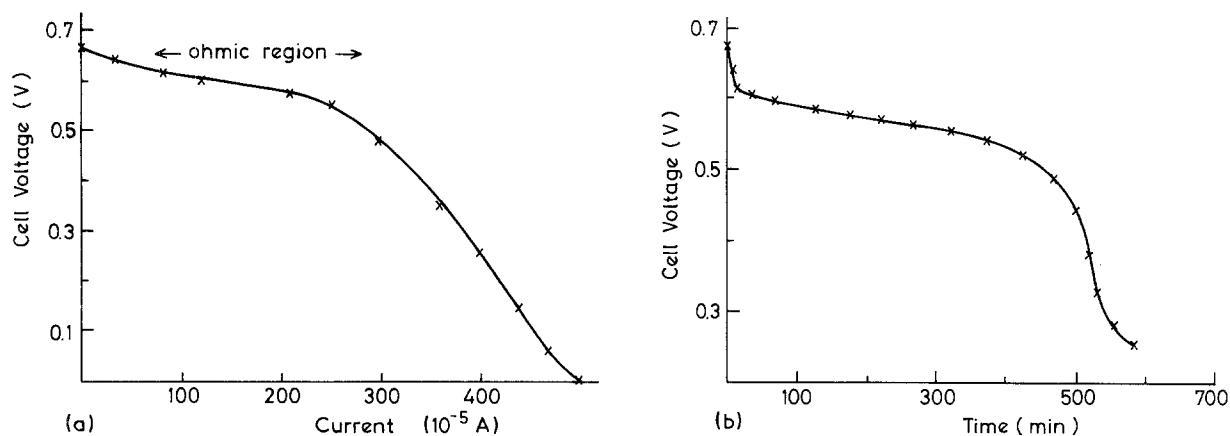


Figure 7 (a) Polarization, (b) discharge (load resistor 2.15 K) characteristics for G10 at room temperature.

TABLE II Cell parameters

Cell weight	1.05 g
Electrolyte thickness	0.10 cm
Electrolyte diameter	1.00 cm
Power density*	0.18 W kg ⁻¹
Energy density*	1.37 Wh kg ⁻¹

*With load resistor 2.15 k Ω .

battery voltage remains constant during the initial period of 450 min and thereafter the voltage drops significantly. A typical cell polarization curve is shown in Fig. 7b. The voltage shown in the figure was measured after 60 sec discharge at each current density. The decrease of voltage at higher current densities could be explained by the anodic and cathodic polarization [25]. The cell parameters are summarized in Table II.

The characteristic performance of the present cell follows the other AgI-based silver electrochemical cells [24–26]. In spite of the high cost of silver–iodine batteries and modest energy values achievable, it is desirable to research further utilizing the advantages of the glassy nature of the solid electrolyte.

5. Conclusion

A glass forming region was found in the undoped and AgI-doped ternary system Ag₂O–MoO₃–V₂O₅. The electrical conductivity of these undoped glasses was investigated with different glass former ratios, and the highest conductivity, $\sigma_{\text{rt}} = 3.21 \times 10^{-6} \Omega^{-1} \text{cm}^{-1}$ was observed when the glass former ratio was unity. The σ_{rt} of the vanadomolybdate glasses increases upon addition of AgI to a maximum value of $2.2 \times 10^{-2} \Omega^{-1} \text{cm}^{-1}$. Although the conductivity of the present glass (G10) remains favourably in the same order, an increase in T_g has been observed in comparison to the 75 AgI 25 Ag₂MoO₄ (mol %) glassy system. The activation energies calculated from the Arrhenius plots for the highly conducting undoped and AgI-doped system were found to be 0.466 eV, 0.153 eV, respectively. The ion hopping rate and relaxation time (derived from modulus peaks) were found to be thermally activated and composition dependent. Finally, the applicability of the highly conducting AgI-doped system as a solid electrolyte in an electrochemical cell was investigated. The cell parameters have been tabulated.

Acknowledgement

The authors wish to thank Mr Hu Peh Yin for carrying out some preliminary work on these glasses as a part of his BSc Honours research programme.

References

1. T. MINAMI, H. NAMBU and M. TANAKA, *J. Amer. Ceram. Soc.* **60** (1977) 467.
2. M. LAZZARI, B. SCROSATI and C. A. VINCENT, *ibid.* **61** (1978) 452.
3. A. KONE, M. RIBES and J. L. SOUQUET, *Phys. Chem. Glasses* **23** (1982) 18.
4. G. CHIODELLI, A. MAGISTRIS and M. VILLA, *Solid State Ionics* **18, 19** (1986) 356.
5. A. MAGISTRIS, G. CHIODELLI and M. DUCLOT, *ibid.* **9, 10** (1983) 611.
6. B. V. R. CHOWDARI and R. GOPALAKRISHNAN, S. H. TANG and M. H. KUOK, *Solid State Ionics*, in press.
7. B. CARETTE, E. ROBINEL and M. RIBES, *Glass Technol.* **24** (1983) 157.
8. T. MINAMI, H. NAMBU and M. TANAKA, *J. Amer. Ceram. Soc.* **60** (1977) 283.
9. B. V. R. CHOWDARI and R. GOPALAKRISHNAN, *Solid State Ionics* **18, 19** (1986) 483.
10. B. V. R. CHOWDARI and K. RADHAKRISHNAN, *ibid.* **24** (1987).
11. J. E. BAUERLE, *J. Phys. Chem. Solids* **30** (1969) 2657.
12. P. B. MACEDO, C. T. MOYNIHAN and R. A. BOSE, *Phys. Chem. Glasses* **13** (1972) 171.
13. J. C. REGGIAIANI, J. P. MALUGANI and J. BERNARD, *J. Chim. Phys.* **75** (1978) 849.
14. T. MINAMI, *J. Non-Cryst. Solids* **79** (1986) 367.
15. A. K. JONSCHER, *Nature* **267** (1977) 673.
16. D. P. ALMOND, C. C. HUNTER and A. R. WEST, *J. Mater. Sci.* **19** (1984) 3236.
17. B. V. R. CHOWDARI and R. GOPALAKRISHNAN, *Solid State Ionics* **23** (1987) 225.
18. D. P. ALMOND, G. K. DUNCAN and A. R. WEST, *J. Non-Cryst. Solids* **74** (1985) 285.
19. F. S. HOWELL, R. A. BOSE, P. B. MACEDO and C. T. MOYNIHAN, *J. Phys. Chem.* **78** (1974) 639.
20. J. WONG and C. A. ANGELL, in "Glass Structure by Spectroscopy" (Marcel Dekker, New York, 1976) Ch. 11, p. 740.
21. S. W. MARTIN and C. A. ANGELL, *J. Non-Cryst. Solids* **83** (1986) 185.
22. E. ROBINEL, B. CARETTE and M. RIBES, *ibid.* **57** (1983) 49.
23. J. KAWAMURA and M. SHIMOJI, *ibid.* **79** (1986) 367.
24. T. MINAMI, T. KATSUDA and M. TANAKA, *J. Electroanal. Chem.* **63** (1975) 9.
25. C. A. VINCENT, F. BONINO, M. LAZZARI and B. SCROSATI, in "Modern Batteries" (Edward Arnold, London, 1984).
26. D. W. MURPHY, J. BROADHEAD and B. C. H. STEELE (eds), in "Materials for Advanced Batteries" (Plenum, 1980).

Received 9 March
and accepted 22 September 1987